Use of highly energetic (116 keV) synchrotron radiation for X-ray fluorescence analysis of trace rare-earth and heavy elements

Izumi Nakai[a*], Yasuko Terada[a], Masayoshi Itou[b] and Yoshiharu Sakurai[b]

[a]Department of Applied Chemistry, Science University of Tokyo, Tokyo 162-8601, Japan, [b]SPring-8, JASRI, 1-1-1 Kouto, Mikazuki-cho, Sayo-gun, Hyogo 679-5198, Japan. E-mail: inakai@ch.kagu.sut.ac.jp

This study has revealed the advantages of the use of 116 keV X-rays as an excitation source of X-ray fluorescence (XRF) analyses. This technique is suitable for nondestructive multielemental analyses of heavy elements such as rare-earth elements. The lowest MDL value evaluated for the bulk analysis of a JG-1 standard reference sample (granite rock) was 0.1 ppm for W for a 500 s measurement. The spectrum of standard glass samples of SRM612 demonstrated clearly resolved *K*-line peaks of more than 30 elements, including all the existing rare-earth elements, at 50 ppm levels. The calibration curve for the determination of a rare-earth element shows a linear relation between the XRF intensity and concentrations from 10 to 0.03 ng. This powerful technique should be useful for nondestructive analyses of rare-earth and heavy elements in geological, geochemical and archaeological samples as well as industrial materials.

Keywords: X-ray fluorescence analysis; high energy; rare-earth elements; trace-element analysis; *K*-line analyses; archaeological application.

1. Introduction

X-ray fluorescence (XRF) analysis is widely used in industry as well as in laboratories where X-ray tubes and rotating anodes are used as excitation sources. The development of the synchrotron radiation X-ray source during the past 25 years has opened several new fields of XRF analysis: *i.e.* the utilization of brilliant monochromatic X-rays with linear polarization has resulted in drastic improvements in the detection limits of trace elements and has enabled us to carry out two-dimensional analyses with X-ray fluorescence microprobes using microbeams of a few μm size. In addition, the utilization of the energy tunability of SR X-rays has enabled us to carry out chemical speciation using the X-ray absorption near-edge structure (XANES) technique, and so on (Sparks, 1980; Iida & Gohshi, 1991). These techniques have been developed and established through the use of first- and second-generation synchrotron radiation sources.

Currently, third-generation synchrotron light sources have begun to be constructed. These light sources incorporate insertion devices, wigglers and undulators. The primary characteristics of the third-generation light sources are their extremely high brilliance and the availability of high-energy X-rays. The former characteristic is already well appreciated in relation to the construction of X-ray microscope systems with a beam size of less than 1 μm (Snigirev *et al.*, 1995; Kagoshima *et al.*, 2000) and that of a TXRF system with fg sensitivity (Wobrauschek *et al.*, 1997; Ortega *et al.*, 1998; Sakurai *et al.*, 2001). However, the utilization of high-energy X-rays from third-generation light sources in XRF analyses has remained a challenge.

A typical XRF spectrum of a multi-component material in energy regions of less than 20 keV is usually complicated by an overlap of the *K*, *L* and *M* emission lines of the component elements. In contrast, the XRF spectrum above 20 keV contains only *K* lines; thus the spectrum becomes simple. Therefore, it is thought that the use of the *K*-lines would be ideal for the analysis of heavy elements of atomic number $Z \geqslant 45$ (= Rh $K\alpha_1$ = 20.12 keV). The energy of the *K*-absorption edge of an element increases with the atomic number of the element, and an X-ray energy of 115.62 keV is necessary to excite the U *K*-lines.

Heavy-element analysis using *K*-line spectra was first studied utilizing either first-generation synchrotron light sources such as VEPP-4 in Novosibirsk, USSR (Baryshev *et al.*, 1987; Dar'in & Bobrov, 1987; Khvostova & Trunova, 1987) and HASYLAB in Hamburg, Germany (Janssens *et al.*, 1998), or a second-generation light source at NSLS in Brookhaven (Chen *et al.*, 1993). White X-ray excitation or relatively weak monoenergetic beams with an energy of less than 75 keV have been utilized. Therefore, the intensities of the X-ray sources have not been strong enough to carry out ultra trace-element analysis. Chen *et al.* (1993) have reported MDLs (minimum detection limits) of 6 ppm (La) to 26 ppm (Lu) for a 3600 s counting time when using a wiggler beam. Baryshev *et al.* (1987) have reported an MDL of 50 ppm for the rare-earth elements. Janssens *et al.* (1998) have reported the use of lead-glass capillaries for the microfocusing of highly energetic (>60 keV) synchrotron radiation. With this great improvement in the analytical sensitivity of the focusing optics, they obtained detection limits of 1–10 fg/0.8–2 ppm for the 100 μm silicate samples for the elements from Mn (Z = 25) to Gd (Z = 64) using their *K* lines within a 1000 s counting time.

As for the high-energy X-ray fluorescence analysis utilizing a conventional X-ray source, Harada & Sakurai (1999) have reported in detail the advantages of the use of high-energy X-rays in XRF analysis based on their laboratory data. They constructed a sealed X-ray tube (W anode) system with a high-voltage power supply (160 kV and a maximum load of 1.6 kW for normal focus and of 0.64 kW for fine focus) for high-energy X-ray fluorescence analysis. The detection limit of iodine with regard to concentration was found to be 8 ppm and with regard to an absolute amount to be 3 μg based on the use of a preliminary beam filter technique (80 kV, 18.5 mA). The corresponding values obtained through the use of a white excitation technique (80 keV, 0.6 mA) were 40 ppm and 15 μg. Monochromatic excitation significantly reduced the background signal compared with the white X-ray excitation, and is favorable for the trace element analysis (Harada & Sakurai, 1999).

In the present study we utilized high-energy X-rays from third-generation SR sources. A beamline of the 8 GeV storage ring of SPring-8 is suitable for producing high-energy X-rays up to 300 keV. We have used 116 keV X-rays for the first time as an excitation source in XRF analysis, which allows us to analyze all the heavy elements utilizing a *K* series of emission lines. The purpose of the present study is to examine the potential ability of high-energy XRF analysis and to clarify the analytical characteristics of this new field of XRF analysis.

2. Experimental

The samples included standard reference materials (JG-1: granite rock, Rock Reference samples, Geological Survey of Japan;

SRM612 Trace Elements in Glass Matrices, National Institute of Standards and Technology) and several standard solutions of rare-earth elements with known concentrations. A fine powder (0.2 g) of the rock sample (JG-1) was pressed to form a disk of diameter 10 mm and was placed on a plastic sample holder with adhesive tape. A tiny flake (thickness *ca.* 0.1 mm) of the glass sample (SRM612) was placed directly on the holder with adhesive tape. The calibration standards of various concentrations used to determine sensitivities and to calibrate intensity levels were prepared by diluting a 100 ppm standard solution for atomic absorption spectroscopy with a weak nitric acid solution. Gd was used as an internal standard by adding the solution of Gd to each sample solution. A volume of 1 µl of each internally standardized (the concentration of Gd was kept to 5 ppm) solution was dropped onto a mylar film on the plastic holder. The microdroplets were then vacuum dried. The sample holder was set on the automatic XY stage, and the analysis point was irradiated by a small laser beam and monitored by a video camera. The X-ray beam size was adjusted by a combination of horizontal and vertical slits and was as follows: 1×0.5 mm^2 for JG-1, 0.3×0.3 mm^2 for SRM612, and 1×1 mm^2 for the liquid droplet samples.

The XRF experiments were carried out at SPring-8 utilizing the high-energy X-rays from an elliptical multipole wiggler as an excitation source. The measurements were carried out at a BL08W beamline that was originally constructed for high-energy inelastic scattering experiments. We have newly set up an energy-dispersive XRF analysis system composed of an XY automatic stage (SIGMA KOOKI), a pure-Ge solid-state detector (CANBERRA: GUL0055p), a spectroscopy amplifier (CANBERA 2021: shaping time 12 µs), and a multichannel analyzer (SEIKO EG&G: MCA7700). A full range of the multichannel analyzer was adjusted to 102.4 keV and the energy step was 0.1 keV per channel for the JG-1 and liquid droplet samples and 0.025 keV per channel for the SRM612 glass sample.

A schematic diagram of the experimental system is illustrated in Fig. 1. Monochromatic X-rays of 116 keV were obtained from a doubly bent Si(400) monochromator. The energy resolution, $\Delta E/E$, was 1.25×10^{-3} at 115 keV, and the photon flux was 10^{12} photons s^{-1} (Hara 1998; Sakurai *et al.*, 1999).

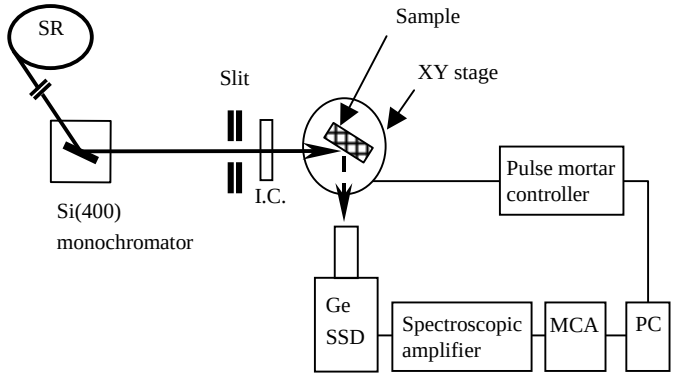

Figure 1
A schematic of the experimental set-up for high-energy XRF analysis at BL-08W of SPring-8.

3. Results and discussion

Fig. 2 shows a typical XRF spectrum of a bulk geological standard sample (JG-1: granite, measurement time 500 s). The certified element concentrations range from 54.7 ppm for Zr down to 1.7 ppm for Er and W. As can be seen in Fig. 2, tungsten as well as various rare-earth elements give distinct *K*-lines. The value of MDL was calculated according to the following equation,

$$\mathrm{MDL} = C * 3\sqrt{I_b} / I_p,$$

where I_b is the background count and I_p is the signal (number of counts) produced by the concentration C (the certified value reported in the reference) of the element. Table 1 shows the values of MDL calculated from Fig. 2 for Fe, Rb, Sr, Zr, Cs, Ba, La, Ce, Nd, Sm, Gd, Dy, Er, Yb, Hf and W together with the certified concentration of each element. The calculated MDL for W in this sample was 0.1 ppm, which is the lowest value of the MDL in Table 1. For the higher-energy region, Compton scattering caused a high background, which deteriorates the signals of low concentration elements. In contrast, the MDL increased with decreases in its energy, which was due to the excitation efficiency. Since the energy of the excited X-ray was 116 keV, which is far from the absorption edge of iron (*ca.* 7 keV), there was a much poorer detection limit for iron (0.097 wt%) than the other heavy elements (see Table 1).

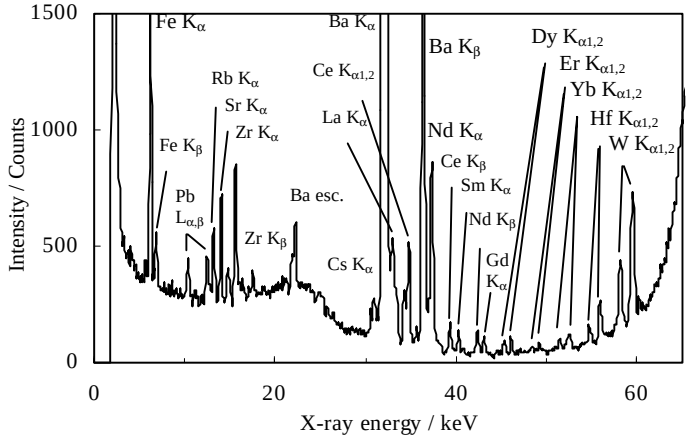

Figure 2
A typical XRF spectrum of geological samples (JG-1, granite rock standard reference sample) excited by 116 keV X-rays and a measurement time of 500 s.

An advantage of the use of high-energy X-rays in XRF analysis is that they have high transmission power (Harada & Sakurai, 1999). The absorption coefficients of the elements sharply decrease with increase in the energy of the X-rays. The mass absorption coefficients of the JG-1 sample were calculated for X-rays with wavelengths of 0.11 Å (113 keV), 0.62 Å (20 keV), 0.21 Å (59 keV, which is equal to the energy of W $K\alpha_1$) and 1.48 Å (8.4 keV, which is equal to that of W $L\alpha_1$) to be 0.16, 3.05, 0.28 and 37.87, respectively, based on the literature data (Sasaki, 1990). These values clearly indicate that the absorption coefficient of the JG-1

Table 1
Minimum detection limit (MDL) values calculated from the XRF spectrum of the JG-1 sample in Fig. 2 for a measurement time of 500 s.

	Contents (ppm)	I_p (counts)	I_b (counts)	MDL (ppm)
Fe	2.02[a)]	1557	366	0.097[a)]
Rb	181	577	281	30.8
Sr	184	719	258	19.2
Zr[b)]	108	395	293.5	54.7
Cs	10.2	280	181	4.2
Ba	462	7205	354.5	3.8
La	23	535	355.5	7.2
Ce	46.6	520	86	3.0
Nd	20	862	154.5	1.1
Sm	5.1	136	45	1.1
Gd	3.7	108	42.5	1.1
Dy	4.6	110	41	1.3
Er	1.7	86	515	1.1
Yb	2.7	125	61	1.0
Hf	3.5	268	98.5	0.6
W	1.7	737	199.5	0.1

[a)] wt%, [b)] K_β

sample for the 20 keV X-rays (3.05), typical energy for conventional SR-XRF analysis, is almost 20 times larger than that for the 113 keV X-rays (0.16). The high-energy X-rays, therefore, have larger penetration depth and are favorable for obtaining bulk chemical composition of a sample. On the other hand, the absorption coefficient of the JG-1 sample for the W $L\alpha_1$ (37.87) line is 135 times larger than that for the W $K\alpha_1$ (0.28) line. This requires smaller absorption correction in a quantitative analysis using the *K* lines of the heavy elements than that using the *L* lines of those elements.

In order to examine the usefulness of the present technique in the analysis of rare-earth elements, we measured the XRF spectrum of a standard SRM612 glass sample. The nominal trace-element concentration of this sample is 50 mg/kg (= 50 ppm) for each of the 61 elements that have been added to the glass support matrix. The XRF spectrum of the sample (counting time: 1000 s) is shown in Fig. 3. It can be seen in the figure that more than 30 heavy elements are clearly detectable, and the peak of each rare-earth element is clearly separated in the spectrum. On the other hand, it is known that the *L*-lines of the rare-earth elements appear from 4.650 keV for La $L\alpha$ to 9.938 keV for Lu $L\beta_2$. There are 15 rare-earth elements (from La to Lu) and 45 peaks ($L\alpha$, $L\beta_1$ and $L\beta_2$ lines for each element if we neglect the $L\gamma$ line) can exist in the XRF spectrum within the small energy region of 5.288 keV (= 9.938–4.650). In addition, the *K*-line spectra of the transition metals from Ti (4.508 keV for $K\alpha$) to Cu (8.040 keV for $K\alpha$) can overlap on the same energy region. Practical samples often contain these transition elements as major components, which disturbs the analysis of the trace heavy elements by *L*-lines. In fact, it has been reported that this SRM612 sample contains Ti, V, Cr, Mn, Fe, Co, Ni and Cu. Therefore it is practically impossible to analyze the rare-earth elements of this glass sample using the *L*-lines by means of the XRF technique. In contrast, in the energy region above 20 keV, there are no peaks other than *K*-lines of the heavy elements. Moreover, the energy difference between La $K\alpha_1$ (33.4418 keV) and Lu $K\alpha_1$ (52.3889 keV) is *ca.* 19 keV, which is large enough to distinguish each rare-earth element under the resolution of a pure-Ge solid-state detector, as is demonstrated in Fig. 3.

Certified values for the rare-earth elements have not been reported for this SRM612 glass, but information values (in ppm) are given as follows. These values are cited in parentheses along with the symbol of the element: Ag(21), Ba(41), La(36), Ce(39), Nd(36), Sm(39), Eu(36), Gd(39), Dy(35), Er(39) and Yb(42). Although this observation is only qualitative, the intensity of the peak of each element in Fig. 3 seems to be consistent with these information values, suggesting that the present technique is applicable to the nondestructive multielemental determination of rare-earth elements as well as other heavy elements such as Hf and Ta at the ppm level.

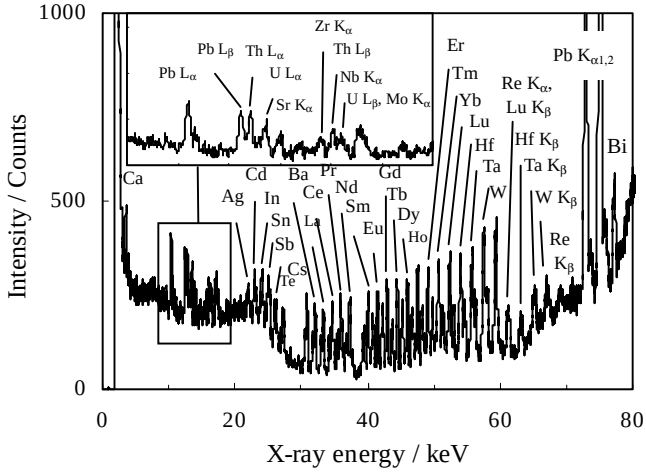

Figure 3
XRF spectrum of a standard SRM612 glass sample showing a good peak separation of the rare-earth elements at 40 ppm levels. The accumulation time is 1000 s.

We also examined the limits of the determination of rare-earth elements by a calibration curve technique using a liquid droplet sample on a mylar film. Lu was used as the target element, and Gd was selected as an internal standard. The net intensities of Lu and Ga were calculated from the measured XRF spectrum, and the former were normalized by the latter value. The normalized intensities were plotted against the absolute amount of Lu. The calibration curve thus obtained from the spectrum with a counting time of 1000 s is shown in Fig. 4. The data show excellent linearity from a Lu level of 10 ng down to 30 pg. The estimated MDL value at the lowest end is 16 pg. These results suggest that a quantitative analysis will be promising for high-energy X-ray fluorescence analysis with proper correction of the matrix effect.

The detection limit of the present technique is largely determined by the degree of elastic and Compton scattering relative to the XRF signal from the analyzed elements. The background counting rate is serious for a bulk sample, and the limit of the counting rate of the detector becomes a dominant factor in determining the detection limit. In fact, we must open the gap of the wiggler to 60 mm in order to measure the bulk sample of JG-1, while the gap should be 40 mm for the measurement of a tiny glass flake of SRM612 and that of a liquid droplet on a mylar film.

Trace-element components of a material often reflect its origin.

Heavy elements in particular are useful as fingerprint elements in provenance analyses of archaeological samples, as heavy elements are trace elements in nature and exhibit unique geochemical behavior because of their large ionic radii and relatively high

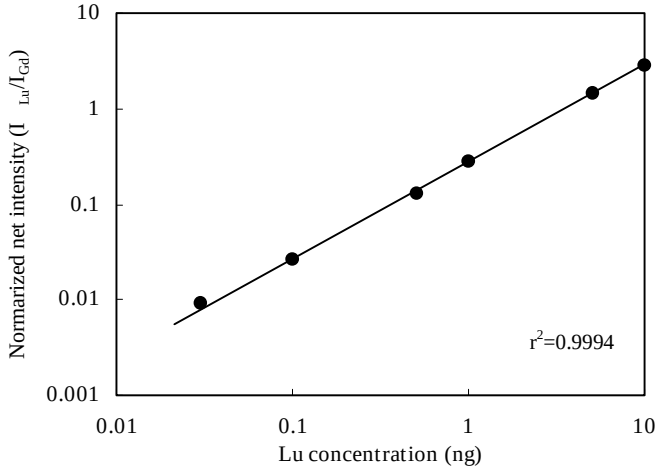

Figure 4
Calibration curves for the determination of Lu. The normalized X-ray intensity of Lu was plotted against the absolute amount of Lu. The XRF intensity of the internal standard of Gd was used in the normalization.

valency. So far, neutron activation analysis has been used for these purposes. However, powder samples are usually necessary for neutron activation analyses, which preclude the analysis of precious samples such as those preserved in museums. Contrastingly, no beam-induced damage of samples was observed throughout the present study, and this technique appears to be truly nondestructive in nature, making it suitable for the analysis of archeological samples. In geochemistry, a chondrite-normalized rare-earth element (REE) pattern is an important indication of the origin of a sample. The present technique allows us to measure the REE pattern directly. Moreover, we can obtain two-dimensional information from a small region of a sample if we use X-ray microbeams obtained by collimators or capillary optics (Haller *et al.*, 1996). In the field of modern industry, rare-earth elements are one of the most important elements used in high-tech materials such as laser, magnetic, fluorescence and superconducting materials. Therefore, the chemical analysis of these elements is an important subject of industrial chemical analysis. However, thus far the analysis of all rare-earth elements has remained difficult. The present technique allows us to analyse all elements with sufficient sensitivity. The minimum detection limit of the current analysis is a sub-ppm level. Accordingly, high-energy XRF analyses will likely become a powerful tool for the analysis of archaeological samples, geochemical samples and high-tech materials containing heavy elements such as rare-earth elements. The utilization of high-energy X-rays from third-generation synchrotron light sources will open new application fields for X-ray fluorescence analyses.

The authors are grateful to Dr T. Ninomiya for his kind help in sample preparation of the XRF experiments. The XRF experiments were performed under the approval of the SPring-8 program Advisory Committee (Proposal No. 1999A0394-UL-np, 1999B0222-NOS-np, 2000A0098-COM-np).

References

Baryshev, V. B., Gil'bert, A. E., Koz'menko, O. A., Kulipanov, G. N. & Zolotarev, K. V. (1987). *Nucl. Instrum. Methods Phys. Res. A*, **261**(1–2), 272–278.

Chen, J. R., Chao, E. C. T., Back, J. M., Minkin, J. A., Rivers, M. L., Sutton, S. R., Cygan, G. L., Grossman, J. N. & Reed, M. J. (1993). *Nucl. Instrum. Methods Phys. Res. B*, **75**(1–4), 576–581.

Dar'in, A. V. & Bobrov V. A. (1987). *Nucl. Instrum. Methods Phys. Res. A*, **261**(1–2), 292–294.

Haller, M., Knochel, A. & Radtke, M. (1996). *HASYLAB Report*, p. 954. HASYLAB, Hamburg, Germany.

Hara, M. (1999). Editor. *Spring-8 Annual Report 1998*, p. 53. Spring-8, JASRI, Hyogo, Japan.

Harada, M. & Sakurai, K. (1999). *Spectrochim. Acta*, B**54**, 29–39.

Iida, A. & Gohshi, Y. (1991). *Handbook on Synchrotron Radiation*, Vol. 4, edited by S. Ebashi, M. Koh & E. Rubenstein, pp. 307–348. Amsterdam: North-Holland.

Janssens, K., Vincze, L., Vekemans, B., Adams, F., Haller, M. & Knochel, A. (1998). *J. Anal. At. Spectrom.* **13**(5), 339–350.

Kagoshima, Y., Takai, K., Ibuki, T., Hashida, T., Yokoyama, Y., Yokoyama, K., Takeda, S., Urakawa, M., Miyamoto, N., Tsusaka, Y. & Matsui, J. (2000). *SPring-8 User Experiment Report, No.5*, p. 436. Spring-8, JASRI, Hyogo, Japan.

Khvostova, V. P. & Trunova, V. A. (1987). *Nucl. Instrum. Methods Phys. Res. A*, **261**(1–2), 295–300.

Ortega, L., Comin, F., Formoso, V. & Stierle, A. (1998). *J. Synchrotron Rad.* **5**, 1064–1066.

Sakurai, K., Eba, H., Inoue, K. & Yagi, N. (2001). *Nucl. Instrum. Methods A*. In the press.

Sakurai, Y., Hiraoka, N., Ito., M., Ohta, T. & Sakai, N. (1999). *SPring-8 User Experiment Report, No.3*, p. 80. Spring-8, JASRI, Hyogo, Japan.

Sasaki, S. (1990). *KEK Report 90*, Vol. 16, pp. 1–142. KEK, Japan.

Snigirev, A., Snigireva, I., Engstroem, P., Lequien, S., Suvorov, A., Hartman, Ya., Chevallier, P., Idir, M. & Legrand, F. (1995). *Rev. Sci. Instrum.* **66**(2,2), 1461–1463.

Sparks, C. J. Jr (1980). *Synchrotron Radiation Research*, edited by H. Winck & S. Doniach, ch. 14. p. 459. New York: Plenum Press.

Wobrauschek, P., Gorgl, R., Kresamer, P., Streli, C., Pahlke, S., Fabry, L., Haller, M., Knochel, A. & Radtke, M. (1997). *Spectrochim. Acta*, B**52**, 901–906.

Received 28 September 2000 • Accepted 16 April 2001